MolecularLibraries
Pathways to Discovery

Probe Report

Title: Discovery of a small molecule inhibitor of ROMK with unprecedented selectivity
Authors: Jerod S. Denton, C. David Weaver, Brain A. Chauder, Craig W. Lindsley* (craig.lindsley@vanderbilt.edu)

Assigned Assay Grant #: NS057041-01
Screening Center Name & PI: Vanderbilt Screening Center for GPCRs, Ion Channels and Transporters, C. David Weaver
Chemistry Center Name & PI: Vanderbilt Specialized Chemistry Center for Accelerated Probe Development, Craig W. Lindsley
Assay Submitter & Institution: Jerod S. Denton, Vanderbilt University

PubChem Summary Bioassay Identifier (AID): 2436

Probe Structure & Characteristics:

2,2′-oxybis(methylene)bis(5-nitro-1*H*-benzo[*d*]imidazole
MW = 368.3, ClogP = 1.96,

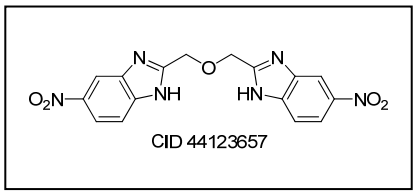

ML112

CID/ML#	Target Name‡	IC50/EC50 (nM) [SID, AID]†	Anti-target Name(s) ‡	IC50/EC50 (μM) [SID, AID]†	Selectivity*	Secondary Assay(s) Name: IC50/EC50 (nM) [SID, AID]§
44123657 ML112	ROMK	220 [84975340,1916,1917]	Kir2.1, Kir4.1, Kir7.1, Kir2.3, PanLabs	> 10 μM [84975340,1916,1924]	>50	Electrophysiology [84975340, 1922]

Recommendations for the scientific use of this probe:

This probe (CID 44123657) can be used for *in vitro* and electrophysiology studies to probe the role of ROMK inhibition without inhibition of closely related channels Kir2.1, Kir4.1, Kir7.1, Kir2.3 or hERG. Moreover a PanLab screen identified no significant ancillary pharmacology, thus CID 44123657 is the first truly selective small molecule inhibitor of ROMK and can be employed to study ROMK with confidence. This is the second probe from this screening effort, the first being CID 4536383, a ROMK inhibitor that is also first known inhibitor of Kir7.1.

Specific AIM: To identify small molecule inhibitors of Renal Outer Medullary Potassium Channel (ROMK, Kir1.1, KCNJ1), a potassium channel located in the renal tubule where it critically regulates sodium and potassium balance. There are no selective small molecule inhibitors of ROMK. We aimed to develop ROMK inhibitors with submicromolar potency, cell penetrance and greater than 10-fold selectivity versus other members of the Kir channel family (Kir2.3, Kir4.1, Kir4.2, Kir5.1 and Kir7.1).

Significance: The Renal Outer Medullary potassium (K) channel (ROMK, Kir1.1, KCNJ1) is expressed in the kidney tubule where it plays key roles in regulating fluid and electrolyte homeostasis.[1,2] In the thick ascending limb of Henle, luminal K recycling by ROMK supports NaCl reabsorption by the Na-K-2Cl co-transporter and loop diuretic (e.g. furosemide) target NKCC2, which in turn promotes osmotic water reabsorption in the distal nephron.[3-5] In the connecting tubule, distal convoluted tubule and collecting duct, ROMK mediates the final step in K secretion and functions to match dietary K intake with urinary K excretion.[6,7] A growing body of genetic evidence[8-10] suggests that pharmacological antagonists of ROMK could have potent diuretic effects while minimizing potentially dangerous urinary K loss caused by furosemide.[11,12] However, the molecular pharmacology of ROMK, and indeed that of the entire inward rectifier K^+ channel family, is virtually undeveloped, precluding assessment of ROMK's potential as a diuretic target.
At least 6 other members (Kir2.3, Kir4.1, Kir4.2, Kir5.1, Kir7.1) of the Kir channel family are expressed in the nephron, but their physiological functions are not well understood.[2,13-16] The newest family member, Kir7.1 (KCNJ13), is expressed in several nephron segments. In principal cells of the collecting duct, Kir7.1 is believed to contribute to basolateral K recycling necessary for Na-K-ATPase-dependent K secretion.[15] However, there is no direct evidence that Kir7.1 forms functional ion channels in the nephron. Kir7.1 has an unusually low unitary conductance (~50 fS),[17] making it difficult to identify in single-channel recordings, and there have been no pharmacological tools available with which to discriminate Kir7.1 from other channels in whole-cell recordings. The identification of pharmacological probes would be helpful in defining the functions of Kir7.1 in the nephron and other tissues.[17,25] To date, there are no potent and or selective ROMK inhibitors; however, known K_{ATP} blockers have been shown to exhibit low potency toward ROMK together with undesirable cardiovascular and metabolic side effects mediated by K_{ATP} channels.[37]

Rationale: In the present study, we developed and implemented a fluorescence-based assay for high-throughput screening (HTS) of chemical libraries for novel modulators of ROMK function, and developed the appropriate counter screens within the Kir family and electrophysiology assays to rapidly confirm and optimize putative ROMK inhibitor hits into selective ROMK inhibitors.[18-25]

Screening Center Information:
Assay Implementation and Screening
PubChem Bioassay Name: Identification of Novel Modulators of ROMK K+ Channel Activity
List of PubChem bioassay identifiers generated for this screening project (AIDs): 1916, 1917, 1918, 1922, 1924, 2436, 2753

PubChem Primary Assay Description: We used C1 cells to develop a fluorescence-based assay of ROMK function for high-throughput screening (HTS). The assay reports flux of the K+ congener thallium (Tl+) through ROMK channels using the fluorescent dye Fluozin-2.[22-24] Figure 1A shows representative fluorescence traces recorded from individual wells of a

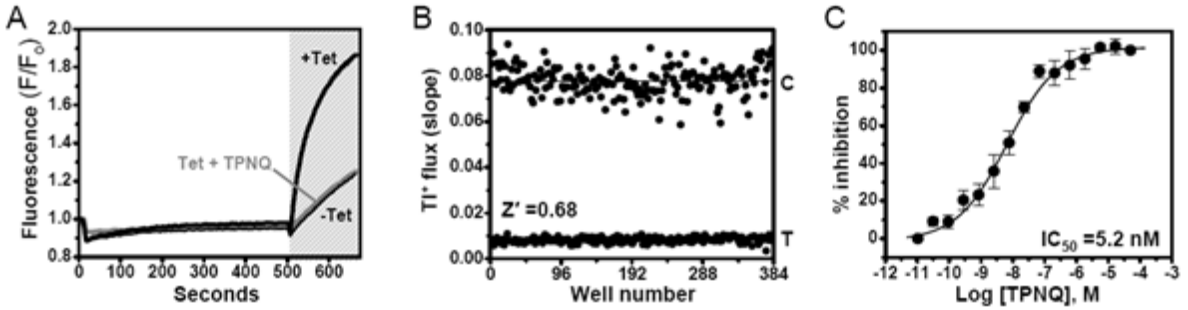

Figure 1. High-throughput assay of ROMK function. (A) Fluozin-2 fluorescence traces recorded from C1 cells before and after addition of extracellular Tl+ (shaded area); (B) Plot of the slope of Tl+-induced fluorescence increase recorded from individual wells of induced C1 cells treated with control buffer (C) or TPNQ (T). The Z' statistic calculated for this plate was 0.68. (C) Concentration-response curve for TPNQ inhibition of ROMK. Data are means □} SEM (n=4). Fit of a 4-parameter logistic function to the CRC data yielded an IC50 of 5.2 nM with 95% confidence intervals between 3.5 nM and 7.6 nM.

384-well plate containing uninduced (-Tet) or Tet-induced cells bathed in control (+Tet) or TPNQ-containing assay buffer (Tet + TPNQ). Tl+ evoked a rapid fluorescence increase in induced cells, but not in uninduced cells or induced cells pre-treated with the ROMK blocker TPNQ. The slope of the Fluozin-2 fluorescence increase between 7 and 12 seconds after Tl+ addition was used as a measure of Tl+ flux. TPNQ dose-dependently decreased Tl+ flux in induced cells with an IC_{50} of 5.2 nM (**Fig. 1C**), indicating the assay is sensitive and capable of reporting graded changes in ROMK activity. To assess the suitability of the assay for HTS, every other well of a 384-well plate was pre-treated with control assay buffer or TPNQ-containing buffer before Tl+ addition. The rate of Tl+ flux varied little within treatments, but was dramatically different between control- and TPNQ-treated wells (**Fig. 1B**). For this plate the calculated Z' value, a statistical indicator of the assay's ability to correctly identify hits in a screen, was 0.68. Assays with Z' values between 0.5 and 1.0 are considered suitable for HTS.[26]

Center Summary of Screen: We developed a robust HTS assay for small-molecule ROMK modulators, which enabled the identification of a novel blocker of ROMK and Kir7.1 channels. The assay extends previous work using Tl+ flux to detect potassium channel and transporter activities[22-25] and overcomes ROMK-specific technical hurdles associated with reportedly poor channel expression in mammalian cells[27-33] by using an inducible expression system and point mutation (S44D) that promotes cell surface expression.[21-35] The identification by HTS of numerous ROMK antagonists, some of which preferentially block other Kir channels, is a significant step toward developing the molecular pharmacology of the inward rectifier channel family. Using the Tl+ flux assay we screened 126,009 compounds in 384-well plates at a single dose of 10 μM. DMSO at a final concentration 0.1% was used as the compound vehicle. During assay development, we established that Tl+ flux through ROMK was insensitive to DMSO concentrations up to 10% (data not shown). Four rows in each plate were filled with control or TPNQ-containing buffer for determination of Z' (e.g. Fig. 3C). Plates with Z' values less than 0.45 were not included in the data analysis.

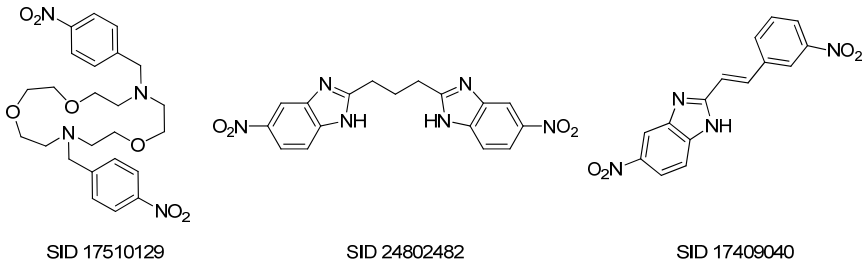

Figure 2. Confirmed ROMK HTS hits

The mean ± SD Z′ of plates passing quality control was 0.72 ± 0.08. The processed primary data resulted in 1,758 compounds designated as inhibitors. After re-orders from ChemDiv and confirmation screening in electrophysiology experiments, we were left with three hits (**Figure 2**): SID 17510129 (IC_{50} = 3 μM), SID 24802482 (80% block @ 10 μM) and SID 17409040 (30% block @ 10 μM).

The first probe from this effort was based on SID 17510129. Resynthesis of the parent in the context of a small parallel library,[36] resulted in 'flat' SAR, but fresh powder of analytically pure SID 17510129/CID 4536383 generated a ROMK inhibitor with an IC_{50} of 294 nM, with selectivity versus Kir2.1 and Kir4.1. However, CID 4536383 was also the first reported small molecule inhibitor of Kir7.1 (70%@ 10 μM).[25] In order to truly probe the role of ROMK and determine therapeutic potential of ROMK inhibition, a more selective ROMK inhibitor was required.

Chemical Probe Lead Optimization: Efforts focused on SID 24802482, a bis-benzimidazole tethered by a propyl chain that displayed 80% inhibition of ROMK at 10 μM. The parent molecule was resynthesized by heating a suspension of glutaric acid **1** and 4-nitrobenzene-1,2-diamine **2** in 5 N HCl in a sealed tube at 120 °C to provide CID 3096126 (SID 24802482) in 48% isolated yield (**Scheme 1**), which was assigned a new SID for this new lot SID 84975339. When evaluated in the Tl^+ assay, fresh powder of analytically pure CID 3096126 possessed an IC_{50} of 60 μM for inhibition of ROMK. This was concerning as the HTS stock afforded 80% inhibition at 10 μM. Upon LCMS inspection of the original HTS DMSO stock solution, we found that the sample contained several impurities. However, we noticed a structural similarity between CID 3096126 and the first generation ROMK probe CID 4536383 (**Figure 3**). Our initial thought on CID 4536383, based on a kryptofix scaffold, was that it chelated potassium ions (K^+). We postulated that if we replaced the central methylene moiety of CID 3096126 with an oxygen atom, we would enhance its ability to chelate K^+ through a three-point chelate **3**, and therefore increase inhibition of ROMK. In order to test this hypothesis, we synthesized **3** by heating a suspension of diglycolic acid **4** and 4-nitrobenzene-1,2-diamine **2** in 5 N HCl in a sealed tube at 120 °C to provide **3**, CID 44123657 (SID 84975340) in 51% isolated yield (**Scheme 2**). When evaluated in the Tl^+ assay, fresh powder of analytically pure CID 44123657 possessed an IC_{50} of 220 nM for inhibition of ROMK, an increase in ROMK potency of over >250-fold (**Figure 4A**).

Scheme 1. Resynthesis of SID 24802482, i.e., CID 3096126

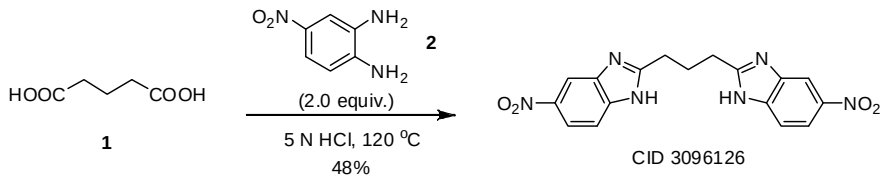

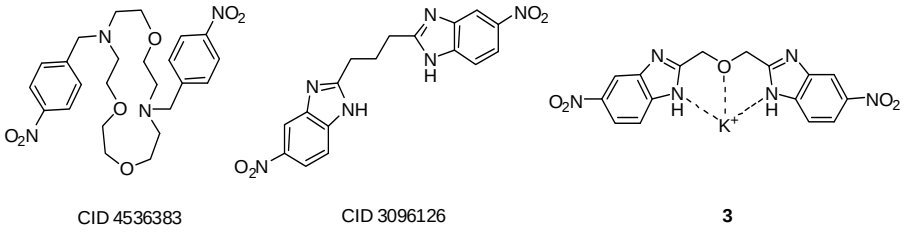

Figure 3. Structural similarities betwen CID 4536383 and CID 3096126: K^+ chelation as a basis for ligand design

Scheme 2. Synthesis of **3**, CID 44123657

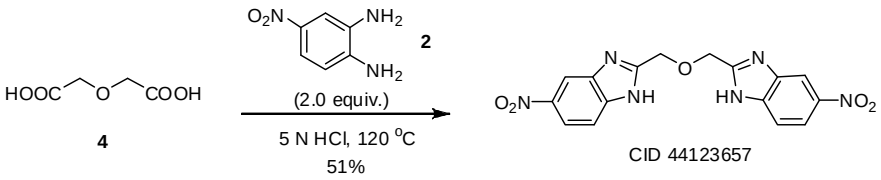

With a new compound that possessed ROMK potency (IC_{50} = 220 nM) acceptable as an MLPCN probe, we next evaluated selectivity versus the Kir family of potassium channels (**Figure 4B**). CID 44123657 was found to possess unprecedented selectivity among the Kir family, having no inhibition of Kir2.1, Kir2.3, Kir4.1, or Kir7.1 at 10 μM drug concentrations, and was thus, not a promiscuous K^+ chelator. In contrast, the first ROMK probe, CID 4536383, displayed considerable inhibition of Kir7.1.[25]

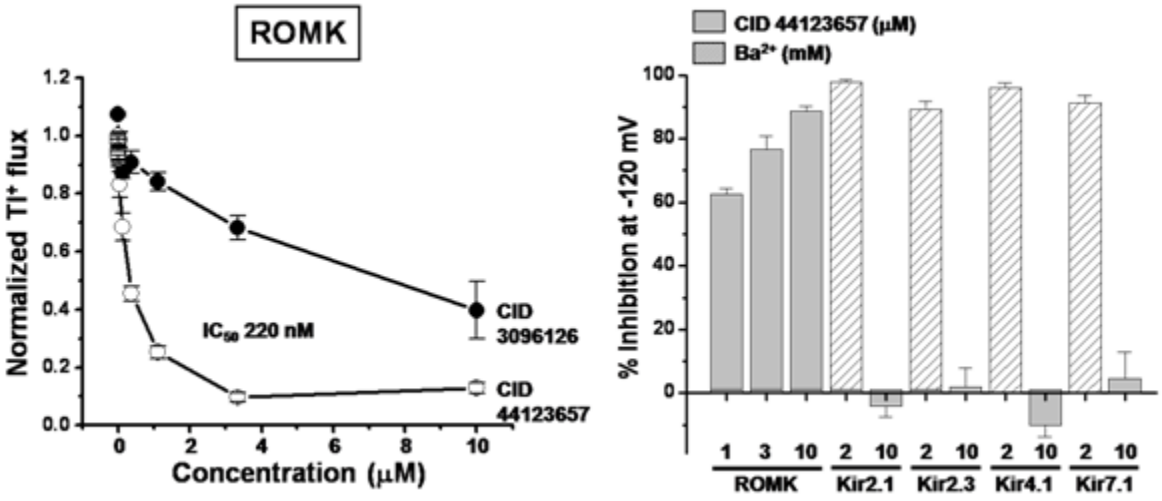

Figure 4. A) CRCs for hit CID3096126 and optimized probe CID44123657; B) Kir family selectivity of CID44123657, the most selective ROMK inhibitor known to date.

The SAR of CID 44123657 was focused around exploring the central carbon linker and the phenyl ring substituents (**Table 1**). Surprisingly, all of the phenyl ring groups that were evaluated were uniformly inactive. In addition, removal of one of the nitro groups from CID 44123657 was not tolerated and led to a complete loss in activity. Without knowing the binding mode for this series of inhibitors, it is difficult to speculate the role the nitro groups are playing.

Table 1. Structures and ROMK Activities of Analogs CID 44123657.

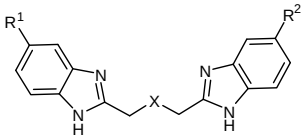

Compound	R^1	R^2	X	IC_{50},μM[a]
CID3096126	NO_2	NO_2	CH_2	4
CID44123657	NO_2	NO_2	O	0.24
CID45259136	F	F	O	<5%[b]
CID2772764	H	H	O	<5%[b]
CID15301607	NO_2	H	O	<5%[b]
CID45259137	SO_2NMe_2	SO_2NMe_2	O	<5%[b]

[a] IC_{50} data are an average of at least three independent experiments using C1 cells in a Tl^+ flux assay
[b] % inhibition of Tl^+ flux at 10μM concentration of compound

At this point, the Lead Profiling Screen (68 GPCRs, ion channels and transporters) from MDS Pharma was performed on CID 44123653 to determine a broader ancillary pharmacology profile for this MLPCN probe. In addition to selectivity versus the Kir family, CID 44123653 possessed clean ancillary pharmacology (**Table 2**), displaying inhibition of only 4 targets:

Table 2. MDS Pharma Lead Profiling Screen for CID 44123653.

Target	Species	% inhibition (10 mM) CID 44123657	Target	Species	% inhibition (10 mM) CID 44123657
Adenosine A1	human	14	Histamine H_3	human	-13
Adenosine A2	human	13	Imidazoline I_2 Central	rat	0
Adenosine A3	human	21	Interleukin IL-1	mouse	-3
Adrenergic α_{1A}	rat	6	Leukotriene, Cysteinyl CysLT$_1$	human	0
Adrenergic α_{1B}	rat	5	Melatonin MT$_1$	human	0
Adrenergic α_{1D}	human	10	Muscarinic M_1	human	2
Adrenergic α_{2A}	human	14	Muscarinic M_2	human	4
Adrenergic β_1	human	6	Muscarinic M_3	human	-4
Adrenergic β_2	human	9	Neuropeptide YY_1	human	5
Androgen (testosterone)AR	rat	10	Neuropeptide YY_2	human	-1
Bradykinin B_1	human	14	Nicotinic Acetylcholine	human	-3
Bradykinin B_2	human	-16	Nicotinic Acetylcholine α_1, Bungarotoxin	human	13
Calcium channel L-type, benzothiazepine	rat	22	Opiate δ (OP1, DOP)	human	-13
Calcium channel L-type, dihydropyridine	rat	26	Opiate κ (OP2, KOP)	human	18
Calcium channel N-type	rat	0	Opiate μ (OP3, MOP)	human	15
Dopamine D_1	human	-2	Phorbol Ester	mouse	-6
Dopamine D_{2S}	human	-6	Platelet Activating Factor (PAF)	human	5
Dopamine D_3	human	1	Potassium Channel [K_{ATP}]	hamster	-6
Dopamine $D_{4.2}$	human	75	Potassium Channel hERG	human	43
Endothelin ET_A	human	0	Prostanoid EP_4	human	10
Endothelin ET_B	human	2	Purinergic P_{2X}	rabbit	-2
Epidermal Growth Factor (EGF)	human	5	Purinergic P_{2Y}	rat	10
Estrogen ERα	human	1	Rolipram	rat	-2
G protein-coupled receptor GPR103	human	15	Serotonin (5-Hydroxytryptamine) 5-HT_{1A}	human	14
GABA$_A$, Flunitrazepam, central	rat	77	Serotonin (5-Hydroxytryptamine) 5-HT_3	human	9
GABA$_A$, Muscimol, central	rat	-3	Sigmaσ_1	human	21
$GABA_{B1A}$	human	0	Sigmaσ_2	rat	18
Glucocorticoid	human	3	Sodium Channel, Site 2	rat	28
Glutamate, Kainate	rat	2	Tachykinin NK_1	human	4
Glutamate, NMDA, Agonism	rat	5	Thyroid Hormone	rat	5
Glutamate, NMDA, Glycine	rat	5	Transporter, Dopamine (DAT)	human	59
Glutamate, NMDA, Phencyclidine	rat	0	Transporter, GABA	rat	16
Histamine H_1	human	13	Transporter, Norepinephrine (NET)	human	56
Histamine H_2	human	0	Transporter, Serotonin (5-Hydroxytryptamine) (SERT)	human	1

Dopamine D_4 (75% @ 10 μM), $GABA_A$ (77% @ 10 μM), DAT (59% @ 10 μM) and NET (56% @ 10 μM). Upon obtaining full CRCs for these four off-target activities, only $GABA_A$ proved to afford an IC_{50}<10 $_m$M ($GABA_A$ IC_{50} = 6.2 μM), 28-fold selective for ROMK. Notably, CID 44123653 was also inactive on hERG and both L- and N-type calcium channels in this panel. Thus, CID 44123652, a ROMK inhibitor with unprecedented selectivity was declared an MLPCN probe for studying the selective inhibition of ROMK *in vitro*.

Solubility: ~ 100 μM in DMSO. Homogeneous/microsuspension at 10 mg/mL in : 20% β-cyclodextrin, 10% cremaphor, 40% PEG-400/H_2O

Synthetic procedure and Spectral data for CID 44123653.

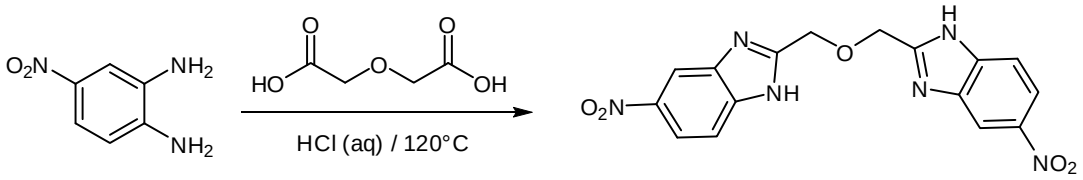

2,2'-oxybis(methylene)bis(5-nitro-1*H*-benzo[*d*]imidazole) (CID 44123652) [ML112]. A suspension of 4-nitrobenzene-1,2-diamine (300 mg, 1.96 mmol) and diglycolic acid (131 mg, 0.98 mmol) in 5N HCl (2 mL) was heated to 120 °C (bath temp) in a sealed tube. A solution forms in 1 h. After 12 h of heating, the mixture was cooled to rt and poured into sat. $NaHCO_3$ solution (50 mL) and the pH was adjusted to 8. The mixture was filtered and the product was washed with water. The product was dried in a vacuum

oven for 10 h to afford CID 44123652 as a light brown solid (368 mg, 51%). The product was recystallized from absolute EtOH to give CID 44123652 as a colorless solid. ^{1}H NMR (400 MHz, DMSO-d_6) δ 8.46 (*d*, *J*=1.3 Hz, 2H), 8.11 (*dd*, *J*=8.8, 1.3 Hz, 2H), 7.73 (*d*, *J*=8.8 Hz, 2H), 5.00 (*s*, 4H); HRMS (calculated for $C_{16}H_{12}N_6O_5$+H) 369.0947; Found 369.0947.

MLS#s: 002474508 (CID 44123652, 500 mg), 002474507, 002765794, 002765793, 002765792, 002765791

Bibliography

1. Wang W, Hebert SC, & Giebisch G *Annual.Review.of Physiology 1997.* 59, 413-436.
2. Hebert SC, Desir G, Giebisch G, & Wang W (2005) *Physiol Rev* 85, 319-371.
3. Hebert SC, Friedman PA, & Andreoli TE (1984) *J Membr Biol* 80, 201-219.
4. Hebert SC & Andreoli TE (1984) *J Membr Biol* 80, 221-233.
5. Hebert SC (1998) *Am.J.Physiol.(Renal Physiol.44)* 275, F325-F327.
6. Frindt G, Shah A, Edvinsson J, & Palmer LG (2009) *Am J Physiol Renal Physiol* 296, F347-354.
7. Wang WH & Giebisch G (2009) *Pflugers Arch* 458, 157-168.
8. Simon DB, Karet FE, Rodriguez-Soriano J, Hamdan JH, DiPietro A, Trachtman H, Sanjad SA, & Lifton RP (1996) *Nat Genet* 14, 152-156.
9. Ji W, Foo JN, O'Roak BJ, Zhao H, Larson MG, Simon DB, Newton-Cheh C, State MW, Levy D, & Lifton RP (2008) *Nat Genet* 40, 592-599.
10. Tobin MD, Tomaszewski M, Braund PS, Hajat C, Raleigh SM, Palmer TM, Caulfield M, Burton PR, & Samani NJ (2008) *Hypertension* 51, 1658-1664.
11. Grobbee DE & Hoes AW (1995) *J Hypertens* 13, 1539-1545.
12. Macdonald JE & Struthers AD (2004) *J Am Coll Cardiol* 43, 155-161.
13. Welling PA (1997) *Am J Physiol* 273, F825-836.
14. Lachheb S, Cluzeaud F, Bens M, Genete M, Hibino H, Lourdel S, Kurachi Y, Vandewalle A, Teulon J, & Paulais M (2008) *Am J Physiol Renal Physiol* 294, F1398-1407.
15. Ookata K, Tojo A, Suzuki Y, Nakamura N, Kimura K, Wilcox CS, & Hirose S (2000) *J Am Soc Nephrol* 11, 1987-1994.
16. Lourdel S, Paulais M, Cluzeaud F, Bens M, Tanemoto M, Kurachi Y, Vandewalle A, & Teulon J (2002) *J Physiol* 538, 391-404.
17. Krapivinsky G, Medina I, Eng L, Krapivinsky L, Yang Y, & Clapham DE (1998) *Neuron* 20, 995-1005.
18. Nadeau H, McKinney S, Anderson DJ, & Lester HA (2000) *J Neurophysiol* 84, 1062-1075.
19. Peters M, Ermert S, Jeck N, Derst C, Pechmann U, Weber S, Schlingmann KP, Seyberth HW, Waldegger S, & Konrad M (2003) *Kidney Int* 64, 923-932.
20. Yoo D, Fang L, Mason A, Kim BY, & Welling PA (2005) *J Biol Chem* 280, 35281-35289.
21. O'Connell AD, Leng Q, Dong K, MacGregor GG, Giebisch G, & Hebert SC (2005) *Proc Natl Acad Sci U S A* 102, 9954-9959.
22. Fallen K, Banerjee S, Sheehan J, Addison D, Lewis LM, Meiler J, & Denton JS (2009) *Channels (Austin)* 3, 57-68.
23. Weaver CD, Harden D, Dworetzky SI, Robertson B, & Knox RJ (2004) *J Biomol Screen* 9, 671-677.
24. Delpire E, Days E, Lewis LM, Mi D, Kim K, Lindsley CW, & Weaver CD (2009) *Proc Natl Acad Sci U S A* 106, 5383-5388.
25. Lewis, L.M.; Bhave, G.; Chauder, B.A.; Banerjee, S.; Lornsen, K.A.; Fallen, K.; Lindsley, C.W.; Weaver, C.D.; Denton, J.S. *Mol. Pharm., in press* (doi: 10.1124/mol.109.059840)
26. Zhang JH, Chung TD, & Oldenburg KR (1999) *J Biomol Screen* 4, 67-73.
27. Schulte U, Hahn H, Konrad M, Jeck N, Derst C, Wild K, Weidemann S, Ruppersberg JP, Fakler B, & Ludwig J (1999) *Proc Natl Acad Sci U S A* 96, 15298-15303.

28. Fakler B, Brandle U, Glowatzki E, Weidemann S, Zenner HP, & Ruppersberg JP (1995) *Cell* 80, 149-154.
29. Lopatin AN, Makhina EN, & Nichols CG (1994) *Nature* 372, 366-369.
30. Lu Z & MacKinnon R (1994) *Nature* 371, 243-246.
31. Wible BA, Taglialatela M, Ficker E, & Brown AM (1994) *Nature* 371, 246-249.
32. Sali A & Blundell TL (1993) *J Mol Biol* 234, 779-815.
33. Shin HG & Lu Z (2005) *J Gen Physiol* 125, 413-426.
34. Brejon M, Le Maout S, Welling PA, & Merot J (1999) *Biochem Biophys Res Commun* 261, 364-371.
35. Yoo D, Kim BY, Campo C, Nance L, King A, Maouyo D, & Welling PA (2003) *J Biol Chem* 278, 23066-23075.
36. Kennedy, J.P.; Williams, L.; Bridges, T.M.; Daniels, R.N.; Weaver, D.; Lindsley, C.W. (2008) *J. Comb. Chem. 10*, 345-356.
37. Clark, M.A.; Humphrey, S.J.; Smith, M.P.; Ludens, J.H. (1993) *J. Pharmaco.l Exp. Ther*. *265*, 933-937.

APPENDIX I

Solubility, Stability and Reactivity data as determined by Absorption Systems

Solubility. Solubility in PBS (at pH = 7.4) for ML 112 was <0.03 µM.

Stability. Stability (at room temperature = 23 °C) for ML 112 in PBS (no antioxidants or other protectorants and DMSO concentration below 0.1%) is shown in the table below. After 48 hours, the percent of parent compound remaining was not reported, but the assay variability over the course of the experiment ranged from a low of 95% (at 2 hours) to a high of 110% (at 1 hour).

	Percent Remaining (%)						
Compound	**0 Min**	**15 Min**	**30 Min**	**1 Hour**	**2 Hour**	**24 Hour**	**48 Hour**
ML 112	100	101	105	110	95	109	---

Reactivity. As assessed through a glutathione (GSH) trapping experiment in phosphate buffered saline (with a substrate concentration of typically 5-50 µM and a GSH concentration of 5 mM, at t = 60 minutes) ML 112 was found to not form any detectable GSH adducts.*

* Solubility (PBS at pH = 7.4), Stability and Reactivity experiments were conducted at Absorption Systems. For additional information see: https://www.absorption.com/site